Quasi-conformal Surface Remeshing

Chi Po Choi, Xianfeng Gu and Lok Ming Lui

Abstract—Curvilinear surfaces in 3D Euclidean spaces are commonly represented by triangular meshes. The quality of the triangulation is important, since it affects the accuracy of the numerical computation on the surface. Surface remeshing refers to the process of optimizing the regularity of the triangulation from an irregular mesh. A popular technique is by conformally parameterizing the surface onto a simple parameter domain. A regular triangulation on the parameter domain is then projected onto the surface through interpolation. For a highly irregular mesh, the conformal parameterization is difficult to compute, causing the technique impractical. This work proposes an effective algorithm to obtain a conformal parameterization of a highly irregular mesh, using quasi-conformal Teichmüller theories. The conformality distortion of an initial parameterization is corrected by a quasi-conformal map, and hence the conformal parameterization can be robustly obtained. However, another major issue is the area distortions introduced under the conformal map. Direct projection of an arbitrary regular mesh may cause a serious loss of geometric details. An adaptive triangulation on the parameter domain is necessary. In this paper, we propose to obtain a regular triangulation on the conformal parameter domain, which is adaptive to the area distortion of the parameterization, through the landmark-matching Teichmüller map. Experiments have been carried out to parameterize and remesh several surface meshes representing real 3D geometric objects using the proposed algorithms. Results show the efficacy of the algorithms to parameterize and optimize the regularity of an irregular triangulation.

Index Terms—Surface remeshing, Teichmüller map, Beltrami holomorphic flow, Beltrami coefficient, conformal, quasi-conformal.

1 Introduction

With the advance of image acquisition technologies, 3D geometric objects from the real world can now be effectively captured. The captured geometric data are commonly represented by triangular meshes. With these digital geometric data, systematic shape analysis of the geometric objects and numerical computations on it can be carried out. Applications can be found in different areas, such as medical imaging, computer graphics and computer visions.

In order to ensure the accuracies of the shape analysis and numerical computations, a high quality triangular mesh that represents the geometric object is crucial. For example, numerical analysts often focus on the mesh quality as it affects the numerical accuracies of the computations. Mesh quality also affects the accuracies of computing geometric quantities, such as curvatures, which further affects the accuracies of shape analysis results. In practical situations, triangulation from 3D raw geometric data are sometimes irregular. It is therefore necessary to develop algorithms to improve the regularity of the triangulation from an irregular mesh. Such as process is called *surface remeshing*.

A commonly used method for surface remeshing is done by surface parameterization. The surface is firstly parameterized onto a simple parameter domain, for instance, a 2D rectangle. A regular triangulation on the parameter domain is then built, which can be projected onto the original surface through interpolation. To preserve the regularity of the triangulation after the projection, the parameterization has to preserve the local geometry as much as possible. A popular choice is the conformal parameterization. For surface meshes satisfying certain regularity conditions, conformal parameterizations can be obtained using conventional parameterization algorithms. However, for highly irregular meshes, conformal parameterizations are generally difficult to compute (see Table 1). As a result, the remeshing algorithm through parameterization becomes impractical. For example, Figure 1 shows two examples of irregular meshes, on which conventional conformal parameterization methods fail.

In this paper, our goal is to develop an effective algorithm to obtain an optimal conformal parameterization of a highly irregular mesh, using quasi-conformal Teichmüller theories. The irregular mesh is firstly embedded in $\mathbb{R}^2$ using the Tutte's embedding. This initial parameterization is expected to introduce conformality distortions. To fix the conformality distortions, the initial parameterization is composed with a quasi-conformal map from the initial parameter domain to the unit disk. An optimal conformal parameterization can be obtained. A regular triangulation on the conformal parameter domain can be built, which is then projected onto the original surface through interpolation. However, one important issue is that the conformal parameterization often introduces area

- *C.P. Choi and L.M. Lui are with the Department of Mathematics, The Chinese University of Hong Kong, Hong Kong.*
- *X.F. Gu is with the Department of Computer Sciences, State University of New York at Stony Brook.*

distortions. When an arbitrary regular mesh on the conformal parameter domain is projected onto the surface, the resolution at some regions may get coarsen. This results in a serious loss in the geometric details (see Figure 7). An adaptive triangulation on the parameter domain is thus necessary. For this purpose, we propose in this work a method to build a regular triangulation on the conformal parameter domain, which is adaptive to the area distortions under the conformal parameterization. The basic idea is to transform a regular mesh with a constrained Teichmüller map (T-Map) that matches landmarks consistently. The landmarks are chosen such that their distribution follows the area distortion of the conformal parameterization. A T-Map is the "most conformal" map subject to the landmark constraints. It transforms the regular mesh to another regular mesh, which follows the area density of the conformal parameter domain. With this triangulation, a remeshed surface can be constructed through interpolation, which keeps the original geometry well. To test the effectiveness of the proposed algorithm, experiments have been carried out on surface meshes extracted from real 3D geometric objects. Results show the efficacy of our proposed algorithm to parameterize and optimize the regularity of an irregular triangular mesh.

In short, the contributions of this paper are two-folded. Firstly, we propose an effective algorithm to robustly compute conformal parameterizations of irregular meshes, even for meshes with highly skinny triangles, using quasi-conformal theories. Secondly, we propose an efficient algorithm to obtain an adaptive regular mesh on the conformal parameter domain based on the area distortion of the parameterization, using the landmark-matching Teichmüller maps (T-Maps). The algorithm also allows us to build subdivision regular meshes of different resolutions to remesh the original surface.

The rest of the paper is organized as follows. In section 2, some related works are presented. In section 3, the basic mathematical background is described. The proposed algorithm for surface remeshing is explained in details in section 4. Experimental results are reported in section 5. The paper is concluded in section 6.

2 Previous work

Surface remeshing is an important pre-processing in computer graphics and scientific computing on surfaces. Many remeshing algorithms have been proposed by various research groups. Existing remeshing algorithms can mainly be divided into two categories, namely, 1. the parameterization approach and 2. the explicit approach. The parameterization approach parameterizes the surface mesh onto a simple parameter domain, on which a structured mesh is built. Surface remeshing is then achieved by projecting the structured mesh onto the surface [5], [4], [3], [6], [8] For example, Praun et al. [5] proposed to remesh genus-0 closed surfaces by mapping it to the spherical domain conformally. Hormann et al. [4] proposed to remesh triangulated topologically disk-like surfaces by parameterizing the surface onto a planar domain, using the most isometric parameterization strategy (MIPS). Eck et al. [3] presented a remeshing algorithm based on partitioning the meshes into several triangular regions followed by parameterizing each regions using harmonic maps. Gu et al. [2] proposed to remesh an arbitrary surface onto a completely regular structure, through cutting the mesh along a network of edge paths, and parametrize the resulting single chart onto a square. Alliez et al. [6] proposed an isotropic remeshing algorithm with locally uniform edges, through building a weighted centroidal Voronoi tessellation in a conformal parameter space, where the specified density function is used for weighting. Later, Alliez et al. [8] proposed an algorithm that uses curvature directions to drive the remeshing process. The algorithm can produce meshes ranging from isotropic to anisotropic, from coarse to dense, and from uniform to curvature adapted.

Another category of remeshing algorithms is the explicit mesh modification approach, in which vertices are progressively adjusted until it matches some specified properties [7], [9], [10], [11], [12], [13], [14], [15], [17]. For example, Peyrè et al. [7] proposed a fast algorithm for the remeshing of a surface with a uniform or adaptive distribution, which is based on iteratively choosing the farthest point according to a weighted distance on the surface. Yan et al. [9] proposed a fast isotropic remeshing method, based on an efficient algorithm for the Restricted Voronoi Diagram (RVD) for computing the centroidal Voronoi tessellation (CVT). Chen et al. [10] proposed a parameterization-free remeshing algorithm by progressively optimizing an initial resampled mesh through alternatively recovering the Delaunay mesh and moving each vertex to the centroid of its 1-ring neighborhood.

In this work, surface remeshing is carried out based on the conformal parameterization. Different algorithms for conformal parameterization has been recently proposed. For instance, Haker et al. proposed a finite element approximation of conformal parameterization in [21]. They linearized the Laplace-Beltrami operator and solved the sparse linear system for conformally parameterizing brain surfaces. In [18], Lévy et al. proposed a parameterization method by approximating the Cauchy-Riemann equations using the least-squares method. Desbrun et al. [19] introduced the intrinsic parameterizations which minimize the distortion of different intrinsic measures of the surface patches. In [20], Hurdal and Stephenson proposed a discrete mapping approach for spherical conformal parameterization which uses circle packing

Fig. 1: Examples of irregular meshes. Conventional conformal parameterization methods fail on these examples.

to produce "flattened" images of cortical surfaces on the sphere, the Euclidean plane, and the hyperbolic plane. Gu and Yau [22], [25] introduced a nonlinear algorithm for spherical conformal parameterization. They performed the optimization in the tangent space of the sphere by gradient descent. The computation is more stable and accurate. In [23], Lai et al. reported an approach to obtain a folding-free global conformal mapping. Curvature flow methods, which deform the Riemannian metric conformally to the uniformization metric, have also recently been studied to obtain conformal parameterizations of surface with arbitrary topologies [26], [28], [29].

Quasi-conformal theories will also be applied in our proposed remeshing algorithm. The computation of quasi-conformal mappings has been recently studied to obtain smooth 1-1 correspondences with bounded conformality distortion [30], [31], [32], [33]. For example, Lui et al. [31] proposed to compute quasi-conformal registration between hippocampal surfaces based on the holomorphic Beltrami flow method, which matches geometric quantities (such as curvatures) and minimizes the conformality distortion [30]. Wei et al. [32] proposed the Quasi-Yamabe flow method to compute quasi-conformal mapping for high-genus surfaces. Quasi-conformal mapping that matches landmarks consistently has also been proposed[30], [34]. In [30], the authors proposed to compute the brain landmark-matching registration, which minimizes L^2 norm of the Beltrami coefficients. Wei et al. [34] also proposed to compute quasi-conformal mappings for feature matching face registration. The Beltrami coefficient associated to a landmark points matching parameterization is approximated. However, either exact landmark matching or the bijectivity of the mapping cannot be guaranteed, especially when very large deformations occur. Later, the extremal QC mapping, which minimizes the conformality distortion has been proposed. Zorin et al. [35] proposes a least square algorithm to compute mapping between connected domains with given Dirichlet condition defined on the whole boundaries. The extremal mapping is obtained by minimizing a least square Beltrami energy, which is non-convex. The algorithm can obtain an extremal mapping when initialization is carefully chosen. Recently, Lui et al. [36] proposed to compute the unique T-Map between simply-connected Riemann surfaces of finite type. The convergence of the algorithm has also been proven in [38]. The proposed algorithm was applied for landmark-based surface registration. Later, Ng et al. [37] extended the algorithm to compute the quasi-conformal extremal map between multiply-connected domains.

3 Basic Mathematical Background

In this work, conformal and quasi-conformal geometry theories will be applied. We describe briefly the basic mathematical theories mostly related to our proposed models in this section. For details, we refer the readers to [24].

Let Ω_1 and Ω_2 be simply-connected domains in $\mathbb{C}$. A map $f : \Omega_1 \to \Omega_2$ is *conformal* if it satisfies the Cauchy-Riemann equation:

$$\frac{\partial u}{\partial x} = -\frac{\partial v}{\partial y}; \ \frac{\partial u}{\partial y} = \frac{\partial v}{\partial x} \tag{1}$$

where $f = u + iv$. In term of metric, a conformal map f preserves the metric up to a multiplicative factor. Mathematically,

$$|dw|^2 = \lambda |dz|^2 \tag{2}$$

where z and w are the coordinates on Ω_1 and Ω_2 respectively. λ is called the *conformal factor*. An immediate consequence of this property is that a conformal map preserves angles. Let S be a Riemann surface. The *conformal parameterization* of S can also be defined. A parameterization $f : S \to \mathbb{C}$ is conformal if every every local chart $\phi : U \subset S \to \mathbb{C}$, $f \circ \phi^{-1} : \phi(U) \subset \mathbb{C} \to \mathbb{C}$ is conformal.

A natural generalization of the conformal map is the *quasi-conformal map*. A quasi-conformal map is an orientation preserving homeomorphism with bounded conformality distortions, in the sense that their first order approximations takes small circles to small ellipses of bounded eccentricity [24]. Mathematically, $f\colon \Omega_1 \to \Omega_2$ is quasi-conformal provided that it satisfies the Beltrami equation:

$$\frac{\partial f}{\partial \overline{z}} = \mu(z)\frac{\partial f}{\partial z}. \tag{3}$$

for some complex-valued function μ satisfying $||\mu||_\infty < 1$. μ is called the *Beltrami coefficient*, which is a measure of non-conformality. μ_f measures how far the map is deviated from a conformal map. $\mu \equiv 0$ if and only if f is conformal. Infinitesimally, around a point p, f may be expressed with respect to its local parameter as follows:

$$f(z) = f(p) + f_z(p)(z + \mu(p)\overline{z}). \tag{4}$$

Obviously, f is not conformal if and only if $\mu(p) \neq 0$. A quasi-conformal map f maps a small circle to a small ellipse. From $\mu(p)$, we can determine the directions of maximal magnification and shrinking and the amount of their distortions as well. Specifically, the angle of maximal magnification is $\arg(\mu(p))/2$ with magnifying factor $1 + |\mu(p)|$; The angle of maximal shrinking is the orthogonal angle $(\arg(\mu(p)) - \pi)/2$ with shrinking factor $1 - |\mu(p)|$. Thus, the Beltrami coefficient μ gives us all the information about the properties of the map. The maximal dilation of f is given by:

$$K(f) = \frac{1 + ||\mu||_\infty}{1 - ||\mu||_\infty}. \tag{5}$$

Given a smooth BC $\mu : \Omega_1 \to \mathbb{C}$ with $\|\mu\|_\infty < 1$. There is always a diffeomorphism of $\mathbb{C}$ that satisfies the equation (3) [24].

4 Proposed algorithm

In this section, we describe our proposed algorithm for surface remeshing in details. The algorithm can be divided into three main steps.

1) Optimal conformal parameterization of an irregular surface mesh: the surface mesh with an irregular triangulation is firstly mapped onto a unit disk using the optimal conformal parameterization.
2) Building an adaptive mesh on the parameter domain: a regular triangulation is built on the conformal parameter domain, which is adaptive to the area distortions under the conformal parameterization.
3) Projection of the regular triangulation to the surface: the adaptive regular triangulation on the parameter domain is projected to the surface through interpolation.

We will explain the procedures in each steps in details.

4.1 Optimal conformal parameterizations of irregular meshes

Suppose K_S is an irregular mesh representing a surface S embedded in $\mathbb{R}^3$. Our goal is to remesh K_S to obtain a regular triangulation representing S. Our strategy is to parametrize K_S conformally and project a regular mesh on the parameter domain back to the original surface through interpolation. However, parameterizing an irregular mesh conformally is challenging. Existing algorithms are sensitive to the quality of the triangulation. For example, for meshes with skinny triangles (that is, one of the three inner angles of the triangle is close to π), the cotangent formula that approximates the Laplace-Beltrami operator usually leads to a singular matrix. As a result, algorithms, which rely on the cotangent formula, would fail on irregular meshes with too irregular triangulation. Figure 1 shows two irregular meshes with skinny triangular faces. Conventional conformal parmeterization methods proposed in [22], [25], [26] and [28] all fail on these two irregular meshes.

To tackle with this problem, we propose an algorithm, under which the numerical computation of the optimal parameterization can be carried out on a regular triangulation. Our strategy is to project K_S to a regular mesh K_Ω in $\mathbb{R}^2$. The projection is not necessarily conformal. The parameterization is then adjusted by computing a quasi-conformal map from K_Ω onto another mesh $K_{\Omega'}$, such that its composition with the initial parameterization becomes conformal.

Denote the collection of vertices of K_S by $V = \{v_i\}_{i=1}^m$; the collection of all edges of K_S by $E = \{e_j\}_{j=1}^n$ and the collection of all faces by $F = \{T_k\}_{k=1}^p$. The conformal parameterization of K_S depends on its angle structure, which captures the information of the angles of each faces. The angle structure depends on the lengths of each edges, which is often called the *discrete metric* defined as follows.

Definition *4.1:* The *discrete metric* on a triangular mesh is a positive real-valued function $l : E \to \mathbb{R}^+$ defined on the collection of all edges that satisfies the following triangle inequality:

$$l([v_i, v_j]) + l([v_j, v_k]) \geq l([v_i, v_k]) \tag{6}$$

where $[u, w]$ denotes the edge joining the vertices $u \in V$ and $w \in V$, and v_i, v_j and v_k forms a triangular face.

The conformal parameterization depends on the discrete metric. An accurate computation of the conformal parameterization relies on the regularity of the triangulation. A triangulation is *regular* if every triangular faces are close to equilateral triangles. In our case, K_S is highly irregular. To find an initial parameterization, we first assign K_S with a fake discrete metric by setting $l \equiv 1$. In other words, we presume all edges have lengths equal to 1. Hence, all triangular faces are presumed to be equilateral.

With this fake metric, we conformally parameterize K_S onto a domain K_Ω in $\mathbb{R}^2$. In this work, we solve the Laplace-Beltrami equation with the fake discrete metric to approximate the parameterization K_S onto the unit disk. This initial parameterization $\varphi : K_\Omega \to K_S$ under the fake discrete metric is also called the *Tutte's embedding*, which is guaranteed to be bijective.

Since all faces of K_S are presumed to be equilateral with the fake discrete metric, most faces are mapped to almost equilateral triangles in $\mathbb{R}^2$ under the Tutte's embedding. Thus, K_Ω is a much more regular triangular mesh in $\mathbb{R}^2$. For example, Figure 4(a) shows the parameterization of the foot mesh with the fake discrete metric, which gives a much more regular triangular mesh of $\mathbb{D}$.

However, under the original discrete metric of K_S, φ is not conformal, since angles are not preserved under the mapping. This is obvious since the triangular faces of K_S are highly irregular, whereas the faces of K_Ω are much more regular. Our goal is to obtain a conformal parameterization of K_S onto a simple domain in $\mathbb{R}^2$.

To obtain such a parameterization, we compose our initial parameterization φ with a quasi-conformal map g that fixes the conformality distortions. More precisely, suppose the Beltrami coefficient of φ is given by μ_φ. Let $g : K_\Omega \to \mathbb{D}$ be a quasi-conformal map with Beltrami coefficient μ_g. Then, the Beltrami coefficient of $\varphi \circ g^{-1}$ is given by:

$$\mu_{\varphi\circ g^{-1}} \circ g = \frac{\mu_{g^{-1}} \circ g + (\frac{g_z}{\overline{g_z}})\mu_\varphi}{1 + (\frac{\overline{g_z}}{g_z})\overline{\mu_\varphi \circ g}\mu_\varphi}. \tag{7}$$

Note that the above formula is valid whenever $||\mu_\varphi||_\infty < 1$. This is guaranteed since φ is a Tutte's embedding, which is bijective. In particular, if g has Beltrami coefficient equals to μ_φ, then

$$\mu_{g^{-1}} \circ g = -(\frac{g_z}{\overline{g_z}})\mu_g = -(\frac{g_z}{\overline{g_z}})\mu_\varphi. \tag{8}$$

Combining Equations (7) and (8), we obtain $\mu_{\varphi\circ g^{-1}} \circ g = 0$. Hence, the composition map $\varphi \circ g^{-1}$ is conformal.

Note that both φ and $\varphi \circ g^{-1}$ are mappings from a 2D domain to the surface K_S in $\mathbb{R}^3$. Their Beltrami coefficients can be computed by locally parameterizing K_S. More specifically, let $D \subset K_\Omega$ and $\gamma : \varphi(D) \to \Sigma \subset \mathbb{R}^2$ be the local chart for $varphi(D)$. Then the Beltrami coefficient of φ on D is defined as the Beltrami coefficient of $\varphi \circ \gamma^{-1}$. We can show that this definition is independent of the choice of γ and hence it is well-defined. The Beltrami coefficient of $\varphi \circ g^{-1}$ can be similarly defined.

Motivated by the above observation, we first compute the Beltrami coefficient μ_φ of the initial parameterization φ. We then compute a quasi-conformal map g from K_Ω to $\mathbb{D}$. The composition map $g \circ \varphi^{-1} : K_S \to \mathbb{D}$ is then a conformal parameterization of K_S. Note that the computation of the quasi-conformal map g is carried out on K_Ω, which is regular. Hence, numerical inaccuracies due to the irregular triangulation (such as skinny triangles) can be avoided.

The associated quasi-conformal map $g : K_\Omega \to \mathbb{D}$ can be obtained by solving the Beltrami's equation:

$$\frac{\partial g}{\partial \bar{z}} = \mu \frac{\partial g}{\partial z} \tag{9}$$

In this work, we apply the Beltrami holomorphic flow (BHF) algorithm to solve Equation (9). We will explain the BHF algorithm briefly. For details, we refer the readers to [37]. The basic idea of the BHF algorithm is to iteratively compute a sequence of mappings converging to our desired quasi-conformal map with the prescribed Beltrami coefficient. In each iteration, the algorithm finds a vector field to deform the mapping, so that its Beltrami coefficient gets closer to the prescribed one. In practice, we choose the initial map as the harmonic map. Suppose $g_n : K_\Omega \to \mathbb{D}$ is obtained at the nth iteration, whose Beltrami coefficient is μ_n. We proceed to look for a mapping g_{n+1}, whose Beltrami coefficient is close to $\nu_n = (1-\epsilon)\mu_n + \epsilon\mu$ ($\epsilon > 0$). Hence, the Beltrami coefficient of g_{n+1} gets closer to the target one. g_{n+1} can be computed as follows. Assume $g_{n+1} = g_n + \mathbf{V}_n$. The variation $\mathbf{V}_n$ can be found by solving the Beltrami equation. It follows from the Beltrami equation that:

$$\mathcal{A}\mathbf{V}_n = -\mathcal{A}g_n. \tag{10}$$

where $\mathcal{A} := \frac{\partial}{\partial \bar{z}} - \nu_n \frac{\partial}{\partial z}$.

In other words, finding $\mathbf{V}_n$ is equivalent to solving the partial differential equation (10) subject to the boundary condition that

$$(g_0 + \mathbf{V}_n)|_{\partial K_\Omega} = \partial \mathbb{D} \tag{11}$$

Note that the point-wise correspondence between ∂K_Ω and $\partial \mathbb{D}$ is not required in (11). Equation (11) simply means $\mathbf{V}_n$ has to be tangential to $\partial \mathbb{D}$. Note that in each step, ϵ can be chosen so that $||\mu_{n+1} - \mu||_\infty$ is minimized. In practice, we choose $\epsilon = 1$. A sequence of quasi-conformal maps $\{g_n\}_{n=1}^\infty$is obtained, whose Beltrami coefficients converge to μ.

Once the quasi-conformal map g is computed, our desired conformal parameterization of K_S can be obtained from the composition map $\phi := \varphi \circ g^{-1} : K_{\Omega'} \to K_S$, where $K_{\Omega'} := g(K_\Omega)$.

Our algorithm to compute a conformal parameterization of an irregular triangular mesh can now be summarized as follows.

Algorithm 1 : *(Conformal parameterization of irregular surface mesh)*
Input : *Irregular triangular mesh:* K_S.
Output : *Conformal parameterization* $\phi : K_{\Omega'} \to K_S$

1) *Compute an initial parameterization* $\varphi : K_\Omega \to K_S$ *of* K_S *with the fake discrete metric* $l \equiv 1$. *Compute the Beltrami coefficient* μ_φ *of* φ.

2) *Using BHF, obtain a quasi-conformal map $g : K_\Omega \to K_{\Omega'}$ with Beltrami coefficient μ_φ.*
3) *Compute the conformal parameterization of K_S by $\phi := \varphi \circ g^{-1}$.*

4.2 Adaptive regular triangulation of the parameter domain

Once the irregular triangular surface mesh is parameterized conformally, a regular triangular mesh can be constructed on the parameter domain. The regular triangulation on the parameter domain can then be projected onto the original surface mesh through interpolation. Since the parameterization is conformal, the regularity of the triangulation is well-preserved. Hence, the original surface can be remeshed to a regular triangular mesh.

However, an important issue is the area distortion under the conformal parameterization. Although a conformal map preserves angles, it does not preserve area. Thus, a large number of triangular faces of the original surface mesh may possibly be squeezed to a small region on the conformal parameter domain (see Figure 4 and 5). If a uniform mesh is built on the parameter domain, some regions would have insufficient faces to approximate the original surface. As a result, geometric features might be lost after remeshing. A regular triangulation of the parameter domain that is adaptive to the area distortion is therefore necessary.

In this work, we propose an algorithm to obtain the adaptive regular triangulation of the parameter domain based on the centroidal Voronoi tessellation and the Teichmüller mapping. We will first briefly describe the centroidal Voronoi tessellation (CVT) and the Teichmüller mapping (T-Map). Our proposed Teichmüller adaptive remeshing algorithm will then be explained in details.

4.2.1 Centroidal Voronoi tessellation (CVT)

In this work, centroidal Voronoi tessellation (CVT) will be used. We explain the concept of CVT briefly. We refer the readers to [39] for details.

CVT is a special kind of Voronoi tessellation. Given a set S and k elements z_i in S $(i = 1, 2, ..., k)$. The idea of Voronoi tessellation is to divide S into k subsets $V_1, V_2, ..., V_k$ such that:

1) $S = \bigcup_{i=1}^{k} \overline{V}_i$ and $V_i \cap V_j = \phi$ if $i \neq j$;
2) $V_i = \{x \in S : d(x, z_i) < d(x, z_j)$ for $j = 1, 2, ..., k,\ j \neq i\}$.

z_i's are called the *generators* and V_i's are called the *Voronoi region* with respect to z_i.

Given a region V in $\mathbb{R}^n$ and a density function $\rho(w)$ defined on V. The *mass centroid* z^* of V is given by:

$$z^* = \frac{\int_V w\rho(w)dw}{\int_V \rho(w)dw}. \tag{12}$$

A centroidal Voronoi tessellation (CVT) is a Voronoi tessellation whose generators z_i's are the same as the mass centroids z_i^*'s of each Voronoi regions V_i's.

The CVT generators are local uniformly distributed according to the density function $\rho(w)$. This property was conjectured by Gersho [40] and was later proven for the 2D cases [41].

CVT is used in this work to find sparse sample points, called *landmarks*, which are distributed according to the area distortion of the conformal parameterization.

4.2.2 Landmark-matching Teichmüller mapping (T-Map)

Teichmüller map (T-Map) is used to project a regular mesh onto the conformal parameter domain. We briefly describe the idea of the T-Map. For details, we refer the readers to [24], [36], [37]

Suppose Ω_1 and Ω_2 are two simply-connected domains in $\mathbb{R}^2$. Let $\{p_i \in \Omega_1\}_{i=1}^n$ and $\{q_i \in \Omega_2\}_{i=1}^n$ be the corresponding landmarks on Ω_1 and Ω_2 respectively. One might be interested in looking for a bijective map $f : \Omega_1 \to \Omega_2$ satisfying $f(p_i) = q_i$ $(i = 1, 2, ..., n)$, which minimizes the conformality distortion. Mathematically, we look for such a landmark-matching bijective map f such that: $||\mu(f)||_\infty \leq ||\mu(g)||_\infty$ over all landmark-matching bijective map $g : \Omega_1 \to \Omega_2$, where $\mu(f)$ and $\mu(g)$ are the Beltrami coefficients of f and g respectively. f is called the *extremal map*.

The extremal map is closely related to the Teichmüller map (T-Map). A T-Map is a quasi-conformal map whose Beltrami coefficient is of the form:

$$\mu = k\frac{\bar{\psi}}{|\psi|}, \tag{13}$$

where $0 \leq k < 1$ is a postive constant, $\psi : \Omega_1 \to \mathbb{C}$ is a holomorphic function on Ω_1. In other words, a T-Map has a uniform conformality distortion ($|\mu| = k$).

Given any prescribed landmark correspondences (say, $\{p_i \in \Omega_1\}_{i=1}^n \leftrightarrow \{q_i \in \Omega_2\}_{i=1}^n$ with $n \geq 3$), there exists a unique T-Map $f : \Omega_1 \to \Omega_2$ satisfying $f(p_i) = q_i$ for $i = 1, 2, ..., n$, which is also the extremal map.

The landmark-matching T-Map is the "most conformal" bijective map satisfying the prescribed landmark constraints. This property is particularly important in our case, since a regular triangulation is required to be mapped to the parameter domain that preserves the angle structure.

4.2.3 Teichmüller adaptive remeshing

We develop a method to build an adaptive mesh on Ω, which is called the *Teichmüller adaptive remeshing*. Our goal is to build a regular mesh on $\mathbb{D}$ according to the area distortion under ϕ. In other words, more vertices are places on regions with larger squeezing.

We start with choosing k landmark points $\{p_i \in K'_\Omega\}_{i=1}^k$ on $K_{\Omega'}$ such that $\{\phi(p_i)\}_{i=1}^k$ are uniformly distributed on K_S. These uniform sampled landmark points give information about the area density of the conformal parameter domain $K_{\Omega'}$. To get the landmark points, our strategy is to apply CVT to get k generators distributed according to the density function, which is given by the area distortion under ϕ. The density function $\rho : K_{\Omega'} \to \mathbb{R}^+$ is defined as:

$$\rho(v_i) = \sum_{T_j \in N(v_i)} \frac{\mathcal{A}(\phi(T_j))}{\mathcal{A}(T_j)}, \tag{14}$$

where $N(v_i)$ is the 1-ring neighbourhood faces of v_i and $\mathcal{A}(T_j)$ is the area of the triangular face T_j. This idea is similar to [7]. However, in this work, only a small amount of sample points (k is much less than the vertex number) are chosen. The sample points are considered as landmarks, which give us information about the area density of the conformal parameter domain. T-Map will then be used to map a regular mesh to the conformal parameter domain that follows the area density based on the landmarks, which significantly speeds up the procedure of building an adaptive mesh on the parameter domain.

We initially take k points on $K_{\Omega'}$ and choose them as the initial generators of the CVT. We then use the Lloyd's method to compute the CVT with respect to the density function ρ, which is a simple iterative scheme as follows:

1) Start with an initial set of k landmark points $\{z_i\}_{i=1}^k$;
2) Construct the Voronoi tessellation $\{V_i\}_{i=1}^k$ of S associated to $\{z_i\}_{i=1}^k$;
3) Construct the mass centroids $\{z_i^*\}_{i=1}^k$ of $\{V_i\}_{i=1}^k$ and set $z_i = z_i^*$ for $i = 1, 2, ..., k$;
4) Go back to Step 2 until convergence.

After the CVT associated to the k generators $\{p_i\}_{i=1}^k$ is computed, the delaunnay triangulation K_{CVT} of $\{p_i\}_{i=1}^k$ can be constructed. K_{CVT} is called the *base mesh*. We then sub-divide K_{CVT} to get a refined mesh $K_{\text{CVT}}^{\text{refine}}$. $K_{\text{CVT}}^{\text{refine}}$ has a good connectivity. However, the triangle quality of it may not be optimized. In some cases, sharp triangular faces may occur (see Figure 4).

To further improve the qualities of the triangular faces, we compute the Tuette's embedding $\Phi : K_{\text{CVT}}^{\text{refine}} \to K_{\text{CVT}}^{\text{tutte}} \subset \mathbb{D}$ from $K_{\text{CVT}}^{\text{refine}}$ into $\mathbb{D}$. A regular triangulation $K_{\text{CVT}}^{\text{tutte}} \subset \mathbb{D}$ of the conformal parameter domain with the same connectivity as $K_{\text{CVT}}^{\text{refine}}$ can be obtained.

Note that the vertex valencies of the subdivision mesh $K_{\text{CVT}}^{\text{refine}}$ are mostly equal to 6. Its Tutte's embedding $\widetilde{K}_{\text{CVT}}^{\text{tutte}}$ gives a regular triangular mesh on the parameter domain $\mathbb{D}$ (see Figure 2). However, the vertices of $\widetilde{K}_{\text{CVT}}^{\text{tutte}}$ does not follow the density function ρ. We propose to deform $\widetilde{K}_{\text{CVT}}^{\text{tutte}}$ to another mesh $\widetilde{K}_{\text{regular}}$ of $\mathbb{D}$, whose vertices follow ρ while preserving the regular angle structure of $\widetilde{K}_{\text{CVT}}^{\text{tutte}}$ as much as possible. Ideally, it is desirable to get a conformal map to deform $\widetilde{K}_{\text{CVT}}^{\text{tutte}}$ according to the density function ρ. But practically, such a conformal map does not exist. Thus, we look for an extremal Teichmüller map, which minimizes the conformality distortion. Mathematically, we search for a diffeomorphism $\mathcal{T} : \mathbb{D} \to \mathbb{D}$ that minimizes $||\mu(\mathcal{T})||_\infty$ while the area density of $\mathcal{T}(\widetilde{K}_{\text{CVT}}^{\text{tutte}})$ resembles ρ as good as possible.

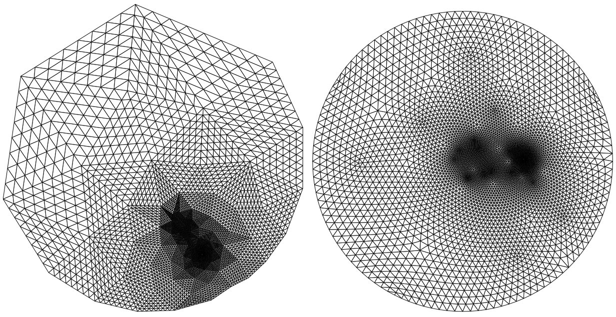

(a) (b)

Fig. 2: (a) Subdivision mesh $K_{\text{CVT}}^{\text{refine}}$ of the base mesh K_{CVT}; (b) Tutte's embedding $\widetilde{K}_{\text{CVT}}^{\text{tutte}}$ of the subdivision mesh.

Note that the k generators give us information about the density of ϕ. The above problem can be solved by finding a landmark-matching T-Map. More specifically, we search for an extremal T-Map $\mathcal{T} : \mathbb{D} \to \mathbb{D}$ satisfying the landmark constraints:

$$\mathcal{T}(\Phi(p_i)) = p_i, \ i = 1, 2, ..., k. \tag{15}$$

$\mathcal{T}$ is then the optimized conformal map to transform $\widetilde{K}_{CVT}^{\text{tutte}}$ to another mesh $\widetilde{K}_{regular} := \mathcal{T}(\widetilde{K}_{CVT}^{\text{tutte}})$ that follows the required density, while preserving the regularity of the triangulation as much as possible. Note again that the extremal T-Map $\mathcal{T}$ is computed on $\widetilde{K}_{CVT}^{\text{tutte}}$, which is regular. The problem of numerical inaccuracies due to irregular triangulation can be avoided.

To compute $\mathcal{T}$, the *Quasi-conformal (QC) iteration* can be used [36]:

1) Start with an initial landmark-matching map $f_0 : \widetilde{K}_{CVT}^{\text{tutte}} \to \mathbb{D}$;
2) Suppose f_n is obtained at the n^{th} iteration. Compute $\nu_n = \mu(f_n)$. Let $\mu_n = \mathcal{L} \circ \mathcal{A}(\nu_n)$, where $\mathcal{A}(\nu) = \frac{\int_\Omega |\nu| dx}{\int_\Omega dx}$ and $\mathcal{L}$ is the Laplace smoothing operator.
   Set $f_{n+1} = \mathbf{LBS}_{LM}(\mu_n)$ where $\mathbf{LBS}_{LM}(\mu_n)$ find the closest landmark-matching map f_{n+1} satisfying the Beltrami equation corresponding to μ_n (in the L^2-sense). More precisely, suppose $\mu_n := \rho_n + i\tau_n$ and $f_n = u_n + iv_n$. The Beltrami equation can be reformulated as follows.

$$\nabla \cdot \left(A \begin{pmatrix} (u_n)_x \\ (u_n)_y \end{pmatrix} \right) = 0; \ \ \nabla \cdot \left(A \begin{pmatrix} (v_n)_x \\ (v_n)_y \end{pmatrix} \right) = 0 \tag{16}$$

where, $A = \begin{pmatrix} \alpha_1 & \alpha_2 \\ \alpha_2 & \alpha_3 \end{pmatrix}$;

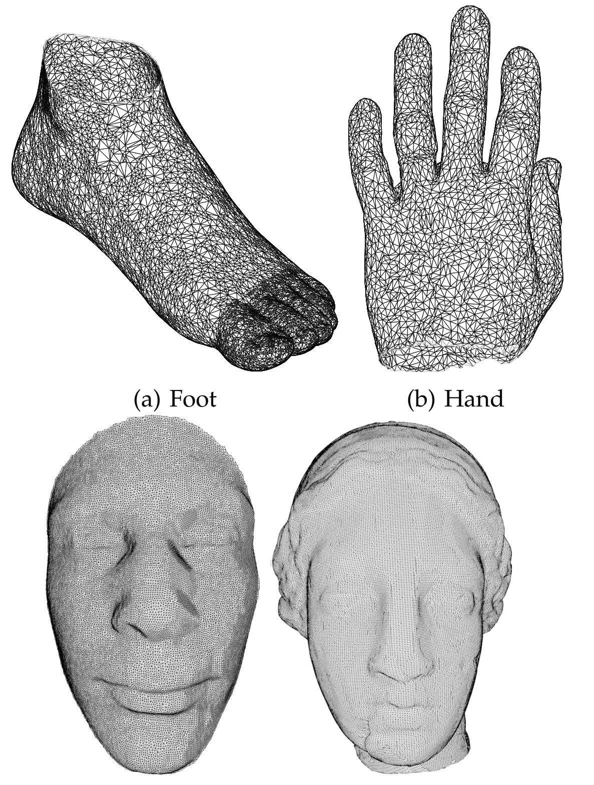

(a) Foot (b) Hand

(c) Human face (d) Venus

Fig. 3: Original surface meshes: Foot, hand, human face and venus.

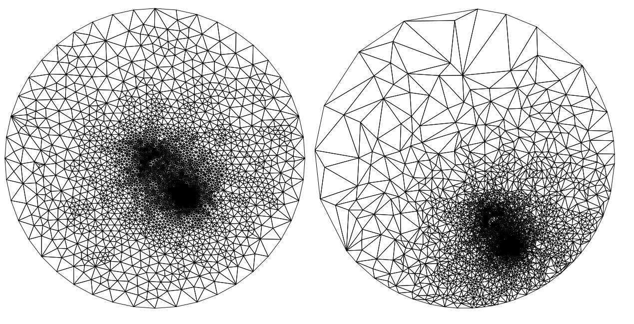

(a) (b)

Fig. 4: Parameterization of Foot: (a) Tutte's embedding and (b) conformal prameterization.

$\alpha_1 = \frac{(1-\rho_n)^2+\tau_n^2}{1-\rho_n^2-\tau_n^2}$; $\alpha_2 = -\frac{2\tau_n}{1-\rho_n^2-\tau_n^2}$; and $\alpha_3 = \frac{(1+\rho_n)^2+\tau_n^2}{1-\rho_n^2-\tau_n^2}$.

Together with the landmark constraints, $\mathbf{LBS}_{LM}$ solves the elliptic PDEs (16) using the least square method.

3) Repeat Step 2 until $||\nu_{n+1} - \nu_n||_\infty < \epsilon$.

The convergence of the above iterative scheme was proven in [38]. Once $\mathcal{T}$ is computed, an adaptive mesh on $\mathbb{D}$ can be constructed, which is given by $\widetilde{K}_{regular} := \mathcal{T}(\widetilde{K}_{CVT}^{\text{tutte}})$.

The proposed Teichmüller adaptive remeshing of the parameter domain can now be summarized as follows.

Algorithm 2 : *(Teichmüller adaptive remeshing)*
Input : *Conformal parameterization* $\phi : K_{\Omega'} \subset \mathbb{D} \to K_S$.
Output : *Teichmüller adaptive mesh* $\widetilde{K}_{regular}$ *on* $\mathbb{D}$

1) *Compute the density function* ρ *of* ϕ
2) *Using CVT with the density function* ρ*, obtain* k *landmark points* $\{p_i \in K_{\Omega'}\}_{i=1}^k$ *such that* $\{\phi(p_i) \in K_S\}_{i=1}^k$ *are uniformly distributed on* K_S*. Construct the delaunnay triangulation* K_{CVT} *of* $\{p_i \in K_{\Omega'}\}_{i=1}^k$.
3) *Refine* K_{CVT} *by subdivision to get* $K_{\text{CVT}}^{\text{refine}}$.
4) *Compute the Tutte's embedding of* $K_{\text{CVT}}^{\text{refine}}$ *into* $\mathbb{D}$ *to obtain* $\widetilde{K}_{\text{CVT}}^{\text{tutte}}$.
5) *Compute the extremal T-Map* $\mathcal{T} : \widetilde{K}_{\text{CVT}}^{\text{tutte}} \to \mathbb{D}$ *such that* $T(\phi(p_i)) = p_i$ *for* $i = 1, 2, ..., k$*. Compute the Teichmüller adaptive mesh* $\widetilde{K}_{\text{regular}} = \mathcal{T}(\widetilde{K}_{\text{CVT}}^{\text{tutte}})$.

The regular mesh $\widetilde{K}_{\text{regular}}$ can then be projected to the surface S using ϕ to get a remeshed surface K^{remesh}. Again, since the parameterization ϕ is conformal, the projected triangulation K^{remesh} is a regular triangular mesh approximating the original surface S. Note also that our proposed Teichmüller adaptive remeshing algorithm involves the subdivision of the base mesh. Our proposed algorithm can easily produce subdivision regular triangulation of various resolutions that remesh the original surface.

4.3 Numerical Implementation

In this subsection, we briefly describe the numerical implementation of the proposed algorithms.

The computation of conformal parameterization of the irregular surface mesh requires approximating the Beltrami coefficient of the initial parameterization φ. The Beltrami coefficient μ is related to the Riemannian metric on S. Suppose S has a metric

$$ds^2 = Edx^2 + 2Fdy^2 + Gdy^2. \tag{17}$$

under the parameterization. Let $dz = dx + idy$ and $\overline{dz} = dx - idy$. The metric can be written as:

$$ds^2 = \lambda|dz + \mu\overline{dz}|^2, \tag{18}$$

where $\lambda = \frac{1}{4}(E + G + 2\sqrt{EG - F^2})$ and $\mu = (E - G + 2iF)/4\lambda$. Hence,

$$\mu = \frac{E - G + 2iF}{E + G + 2\sqrt{EG - F^2}}. \tag{19}$$

Assume that $\varphi(u, v) = (x(u, v), y(u, v), z(u, v))$. Then: $E(u, v) =< (x_u, y_u, z_u), (x_u, y_u, z_u) >$, $F(u, v) =< (x_u, y_u, z_u), (x_v, y_v, z_v) >$ and $G(u, v) =< (x_v, y_v, z_v), (x_v, y_v, z_v) >$. In the discrete setting, $\varphi : K_\Omega \to K_S$ is a piecewise linear homeomorphism. The first order derivatives of x, y and z can be easily computed, which are constants on each triangular faces. E, F, G and hence μ can then be computed. Therefore, in the discrete setting, the Beltrami coefficient is piecewise constant on each triangular face.

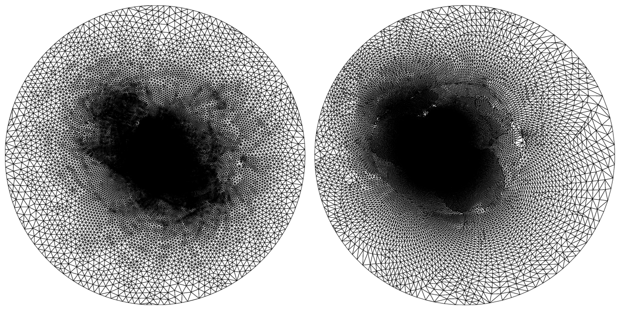

(a) (b)

Fig. 5: Parameterization of Venus: (a) Tuttel embedding and (b) conformal prameterization.

Next, when applying CVT for the Teichmüller adaptive remeshing, the Voronoi tessellation of the k generators has to be computed. To ensure the efficiency, we use a *quantized version* of Voronoi tessellation. Let $\{p_i\}_{i=1}^k$ be the chosen k generators in $\mathbb{D}$. We compute the *quantized Voronoi cell* V_i^q ($1 \leq i \leq k$) as follows:

$$V_i^q := \{v_j \in K_{\Omega'} : d(v_j, v_i) < d(v_j, v_k), 1 \leq j \leq k, j \neq i\}. \tag{20}$$

Besides, the mass centroid z^* has to be computed. Using the integral formula (12) to compute z^* is time-consuming. We simplify the approximation of z^* as follows:

$$z_i^* = \frac{\sum_{v_j \in V_i^q} \rho(z_i) v_j}{|V_i^q| \rho(z_i)}, \tag{21}$$

where $|V_i^q|$ denotes the number of elements in V_i^q.

We leave the details of the numerical implementations for Ricci flow, BHF and QC iterations but refer readers to related references. The numerical implementation for Ricci flow, BHF and QC iterations can be found in [26], [37] and [36] respectively.

5 Experimental Results

We test the proposed remeshing algorithm on different surface meshes embedded in $\mathbb{R}^3$. All our experiments are carried out on a machine with the following configuration: AMD CPU 3.2 GHz and 16GB RAM. The algorithms are implemented using MATLAB. In this section, we report the remeshing results on six surface meshes, namely, 1. foot, 2. hand, 3. human face, 4. Venus, 5. mask and 6. lion. The original surface meshes of 1, 2, 3 and 4 are shown in Figure 3. The original meshes of 5 and 6 are shown in Figure 1. The surface meshes are visualized using the software MeshLab.

5.1 Surface parameterization

We first test Algorithm 1 to parameterize irregular surface meshes. Figure 4 shows the parameterization results of the irregular surface mesh of a foot, whose original surface mesh is shown in Figure 3(a). The Tutte's embedding $\varphi : K_\Omega \to K_S$ is firstly computed by endowing a fake metric (with all edge lengths equal to 1), which is shown in Figure 4(a). Note that the triangulation of the Tutte's embedding K_Ω is regular and has no flipping triangles. From K_Ω, we compute a quasi-conformal map $g : K_\Omega \to K_{\Omega'}$ whose Beltrami coefficient is given by the conformality distortion of φ. The composition map $\phi = \varphi \circ g^{-1}$ is our desired conformal parameterization of K_S, which is shown in Figure 4(b).

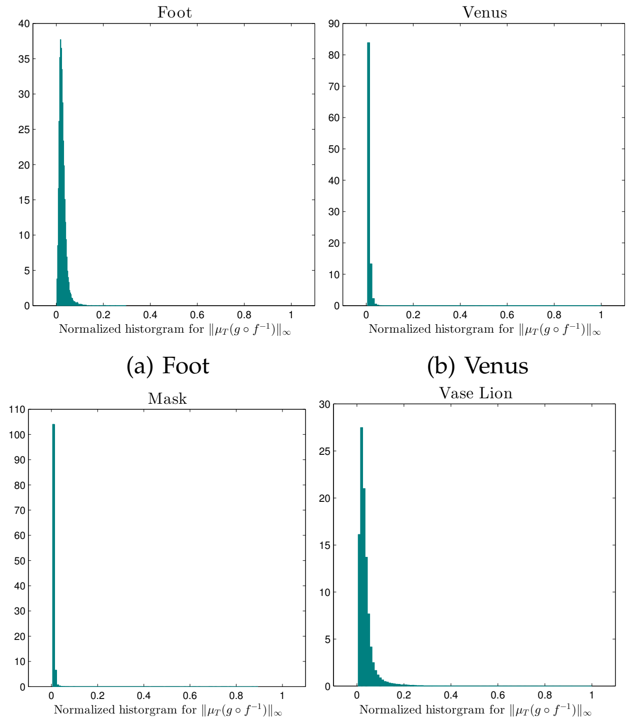

(a) Foot (b) Venus

(c) Mask (d) Lion

Fig. 6: Histogram for $\|\mu(\phi)\|_\infty$

The parameterization results of the irregular surface meshes of Venus are also shown in Figure 5. The Tutte's embeddings are shown in Figure 5(a), which again has no flipping triangle.. The conformal parameterization is shown in Figure 5(b).

Table 1 gives the quantitative comparison of the parameterization results of the six surface meshes with other state-of-the-art approaches. The quantitative measurement is taken as the mean of the Beltrami cofficient of the parameterization. A parameterization is conformal if the value is 0. As shown in the table, our proposed method succeeded in computing the conformal parameterization for all six irregular surface meshes with good conformality. Yamabe flow [27] and inverse distance Ricci flow [28] often fail on the irregular meshes. The conventional Ricci flow [26] is robust in computing the conformal parameterization, however, the conformality is not satisfactory. The double-covering approach, which converts the surface to a genus-0 closed surface and parameterize it using spherical harmonic map (with cotangent formula)[25], is also sensitive to the mesh quality. It fails on the

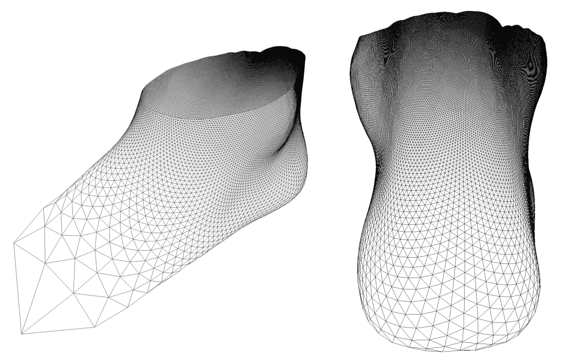

(a) Remeshed foot surface with non-adaptive regular mesh on the parameter domain

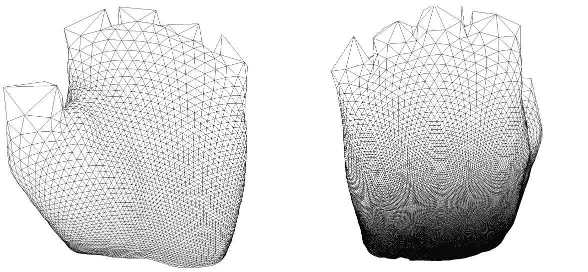

(b) Remeshed hand surface with non-adaptive regular mesh on the parameter domain

Fig. 7: Remeshed surface with a uniform mesh on the parameter domain

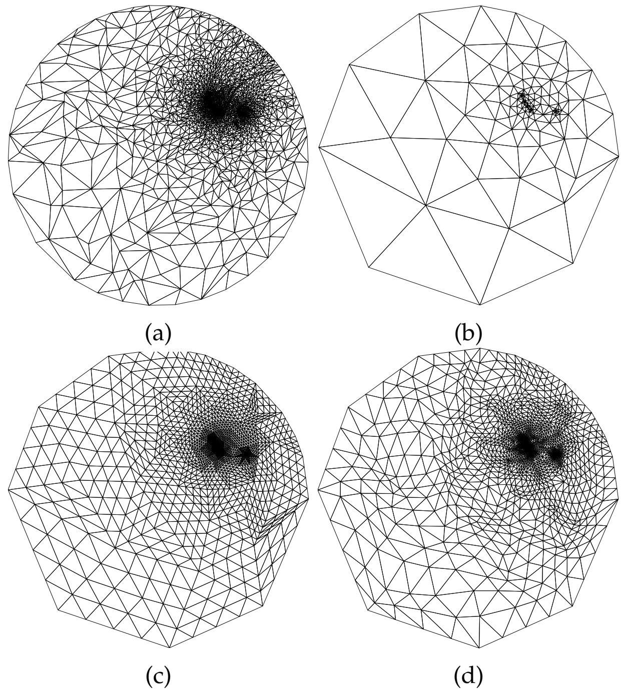

(a) (b) (c) (d)

Fig. 8: Remeshing on the parameterization domain of the hand surface: (a) Parameterization mesh; (b) base mesh; (c) subdivision mesh; (d) Teichmüller adaptive mesh

hand and venus meshes. Also, the conformalities for the successful cases are worse than ours. These experimental results demonstrate that our proposed parameterization method is robust and accurate for computing conformal parameterizations of highly irregular surface meshes.

Mesh	Ricci	Yamabe	IDRF	Double	Ours
Foot	0.2653	0.0238	0.0238	0.0304	0.0247
Hand	0.3328	fail	fail	fail	0.0976
Face	0.2420	fail	fail	0.0679	0.0109
Venus	0.2837	fail	fail	fail	0.0064
Mask	0.2379	fail	fail	0.1104	0.0057
Lion	0.2029	fail	fail	0.0959	0.0323

TABLE 1: The conformality distortion of different parameterization methods.

Figure 6(a), (b), (c) and (d) shows the histograms of the Beltrami coefficient norm for the conformal parameterizations of the foot, Venus, mask and lion respectively. The norms of their Beltrami coefficients are close to 0 for most vertices, illustrating that our proposed algorithm can give good approximations of conformal parameterizations.

5.2 Teichmüller adaptive remeshing

Once the conformal parameterization is obtained, the irregular surface mesh can be remeshed by projecting a regular triangulation on the parameter domain onto the surface using the obtained parameterization. However, the regular mesh on the parameter domain should be adaptive to the area distortion under the conformal parameterization. Otherwise, geometric losses may occur. Figure 7(a) and (b) show the surface remeshing results of the foot and hand respectively by projecting a uniform mesh on $\mathbb{D}$ onto the surfaces. Note that since the uniform mesh on $\mathbb{D}$ is not adaptive to the area distortions of the conformal parameterizations, serious geometric losses near the fingers and toes can be observed.

Figure 8 shows the Teichmüller adaptive remeshing results on the parameter domain of the foot. The conformal parameterization of the foot surface is shown in Figure 8(a). The parameterization is conformal but introduces area distortion. Using CVT, we pick sparse sample points according to the density function on the parameter domain and construct the delaunnay triangulation of the sample points to obtain the base mesh, which is shown in 8(b). In 8(c), we build a denser mesh by subdividing. Note that the geometry of the mesh is not optimized. Some triangular faces have sharp angles. Also, the mesh is not smooth. Jumps across the edges of the base mesh can be obviously seen. Using the T-Map, we compute the Teichmüller adaptive mesh on the conformal parameter domain, which is shown in 8(d). The obtained mesh is comparatively much more regular and smooth.

5.3 Surface remeshing results

With the conformal parameterization and the Teichmüller adaptive mesh on the parameter domain, the regular mesh can be projected onto the surface to obtain a remeshed surface. Figure 9(a) shows the remeshed surface by projecting the base mesh onto the surface. Figure 9(b) is obtained by projecting the subdivision mesh of the base mesh onto the surface. Note that the surface remesh is not smooth. Jumps can be seen across the edges of the base mesh. Figure 9(c) shows our remeshing result of our proposed method. The surface mesh is much more regular and smooth. Figure 10 and Figure 11 show the remeshing results of the foot surface at different viewing angles. The left column shows the original mesh at different angles. The right column shows the remeshed surface at the corresponding viewing angles.

Figure 12 and 13 show the remeshing results of the hand surface at different viewing angles. Figure 14, 15, 16 and 17 show the remeshing results of the face, Venus, mask and lion surfaces respectively. The remeshed surfaces have much better triangle qualities than their original surface meshes.

To quantitatively measure the quality of the remeshing result, we consider a triangle quality measurement, the *radius-ratio* [42]:

$$\tau_i := 2\frac{R_i^{\text{ins}}}{R_i^{\text{cir}}} \qquad \text{for the } i\text{-th triangle in } K_{\text{remesh}} \tag{22}$$

where R_i^{ins} is the radius of the inscribed circle and R_i^{cir} is the radius of the circumscribed circle of the i-th triangle. The radius-ratio τ_i satisfies $0 \leq \tau_i \leq 1$. An equilateral triangle has $\tau_i = 1$ and a degenerated triangle has $\tau_i = 0$. Figure 18, 19 and 20 show the histograms of the radius-ratio for surface meshes of the foot, hand and Venus respectively. (a) show the histogram of the radius-ratio of the original mesh. The histograms of the radius-ratio of the remeshed surfaces using our proposed algorithm are plotted in (d), which shows that most triangular faces have radius-ratio close to 1. It means the triangular meshes are much improved compared to the original mesh.

Fig. 10: Surface remeshing results of the foot surface.

Furthermore, note that our proposed Teichmüller adaptive remeshing algorithm has two major components, namely, 1. the subdivision mesh and 2. the T-Map. In turns out both components are crucial. In fact, building the subdivision mesh helps to improve the triangle qualities of the remeshed surface. (b) show the triangle qualities of the remeshed surfaces obtained by adjusting the vertex positions using CVT and the T-Map while keeping the original mesh topology. The triangle qualities are only slightly improved when compared to the original meshes, and they are in general worse than those obtained by our proposed algorithm. Also, deforming the base mesh using the T-Map benefits for improving the qualities of the triangulations. (c) show the triangle qualities of the surface meshes obtained by projecting the subdivided mesh of the base mesh. Notice that the triangle qualities are not as good as our proposed algorithm.

As for the computational times, for surface meshes with less than 20k faces, the proposed parameterization algorithm takes less than 10s to compute. And the computation for the remeshing algorithm takes less than 2 minutes.

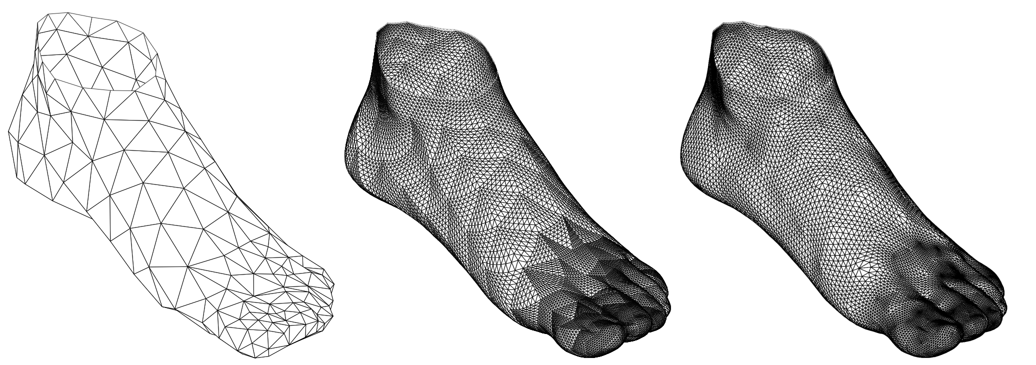

(a) Base mesh (b) Subdivision mesh (c) Teichmüller adaptive mesh

Fig. 9: Remeshing results for the foot surface with different meshes on the parameter domain

Fig. 11: More surface remeshing results of the foot surface at different viewpoint angles.

6 Conclusion

This paper proposes a method for surface remeshing based on quasi-conformal theories. The main idea is to conformally parameterize the irregular surface mesh onto a simple domain. A regular mesh on the parameter domain can then be projected onto the surface using the obtained parameterization. Obtaining conformal parameterization of a highly irregular surface mesh is challenging. In this work, we propose an effective algorithm to obtain optimal conformal parameterizations of highly irregular surface meshes using quasi-conformal Teichmüller theories. After obtaining the parameterization, a regular mesh on the parameter domain, which is adaptive to the area distortion of the parameterization, has to be built. In this work, we propose an algorithm, called the Teichmüller adaptive remeshing, to obtain an adaptive regular mesh on the conformal parameter domain using the landmark-matching Teichmüller map. Experiments have been carried out to remesh several surface meshes, which show the efficacy of the algorithm to optimize the regularity of an irregular triangulation.

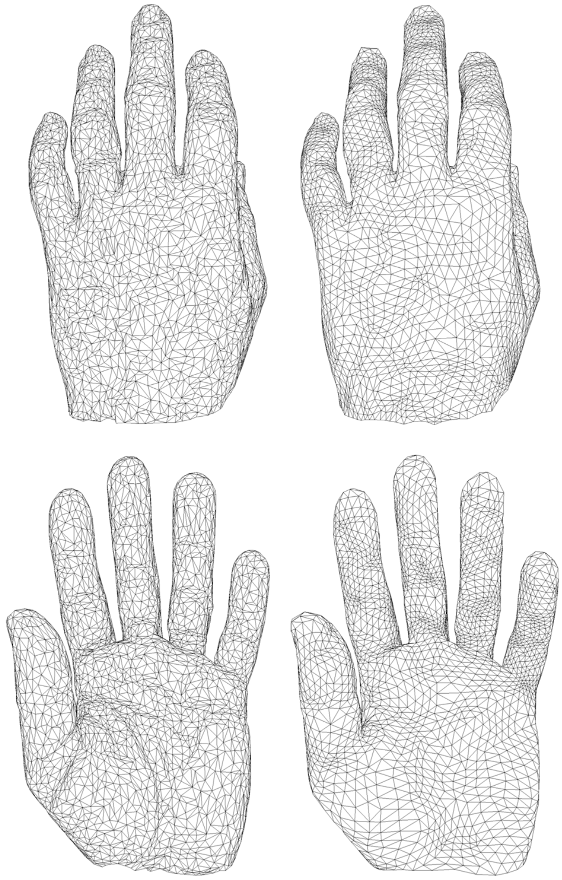

Fig. 12: Surface remeshing results of the hand surface.

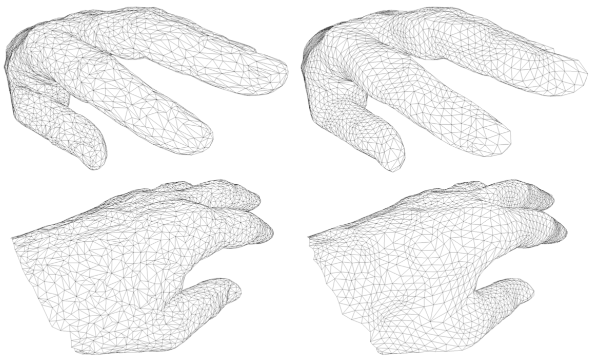

Fig. 13: More surface remeshing results of the hand surface at different viewpoint angles.

References

[1] L.M. Lui, K.C. Lam, S.T. Yau, X.F. Gu *Teichmüller extremal mapping and its applications to landmark matching registration*. arXiv:1211.2569(http://arxiv.org/abs/1210.8025)

[2] X.F. Gu, S.J. Gortler and H, Hoppe *Geometry images*. ACM Transactions on Graphics (TOG) - Proceedings of ACM SIGGRAPH, 21(3), 355-361, 2002

[3] M. Eck, T. DeRose, T. Duchamp, H. Hoppe, M. Lounsbery, and W. Stuetzle *Multiresolution analysis of arbitrary meshes*. ACM Computer Graphics (SIGGRAPH 95 Proceedings), pages 173182, 1995.

[4] K. Hormann, U. Labsik, G. Greiner *Remeshing triangulated surfaces with optimal parameterizations*. Computer-Aided Design, 33(11), 779-788, 2001.

[5] E. Praun, H. Hoppe *Spherical Parametrization and Remeshing*. ACM Transactions on Graphics (TOG) - Proceedings of ACM SIGGRAPH 2003, 22 (3), p. 340-349, July 2003

[6] P. Alliez, E.C. de Verdiere , O. Devillers and Martin Isenburg *Isotropic Surface Remeshing*. Graphical Models, 67(3), 204231, 2005

[7] G. Peyré and L. Cohen *Geodesic Computations for Fast and Accurate Surface Remeshing and Parameterization*. Progress in Nonlinear equation and applications, Vol 63, 157-171, 2005

[8] P. Alliez, D. Cohen-Steiner, O. Devillers, B. Lvy, M. Desbrun *Anisotropic polygonal remeshing*. ACM Transactions on Graphics (TOG), 22(3), 485-493, 2003

[9] D. Yan, B. Lévy, Y. Liu, F. Sun and W. Wang *Isotropic Remeshing with Fast and Exact Computation of Restricted Voronoi Diagram*. Eurographics Symposium on Geometry Processing, Vol 28, 2009

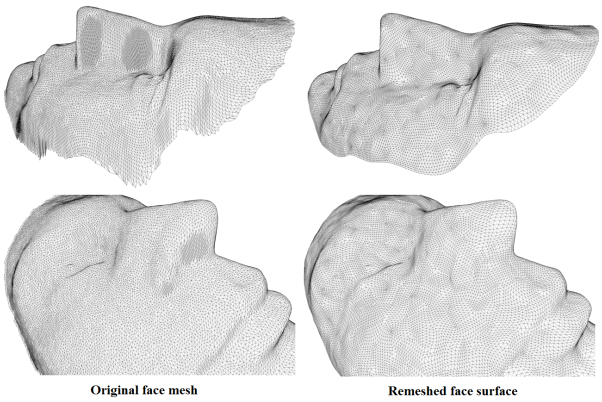

Fig. 14: Surface remeshing results of the human face.

[10] Z. Chen, J. Cao, W. Wang *Isotropic Surface Remeshing Using Constrained Centroidal Delaunay Mesh*. Computer Graphics Forum, 31(7), 20772085, 2012

[11] P. J. Frey *About surface remeshing*. Proceedings of 9th International Meshing Roundtable, 123136, 2000.

[12] P. J. Frey and H. Borouchaki *Geometric surface mesh optimization*. Computing and Visualization in Science, 1:113121, 1998.

[13] H. Hoppe *Progressive meshes*. Computer Graphics. SIGGRAPH 96 Proceedings, 30:99108, 1996.

[14] H. Hoppe, T. DeRose, T. Duchamp, J. McDonald, and W. Stuetzle *Mesh optimization*. Computer Graphics. SIGGRAPH 93 Proceedings, 27:1926, 1993.

[15] A. Rassineux, P. Villon, J.-M. Savignat, and O. Stab. *Surface remeshing by local Hermite diffuse interpolation*. International Journal for Numerical Methods in Engineering, 49:31 49, 2000.

[16] G. Turk. *Re-tiling polygonal surfaces*. Computer Graphics. SIGGRAPH 92 Proceedings, 26:5564, 1992.

[17] Vitaly Surazhsky and Craig Gotsman *Explicit Surface Remeshing*. Computer Graphics. SIGGRAPH 92 Proceedings, 26:5564, 1992.

[18] B. Lévy, and J. Maillot, *Least Squares Conformal Maps for Automatic Texture Atlas Generation*. ACM SIGGRAPH Proceedings (July 2002).

[19] M. Desbrun, P. Alliez, and M. Meyer, *Interactive geometry remeshing*. Proceeding of ACM SIGGRAPH, 2002.

[20] M.K. Hurdal, K. Stephenson, *Cortical cartography using the discrete conformal approach of circle packings*. NeuroImage 23 (2004) S119-S128.

[21] S. Haker, S. Angenent, A. Tannenbaum, R. Kikinis, G. Sapiro,

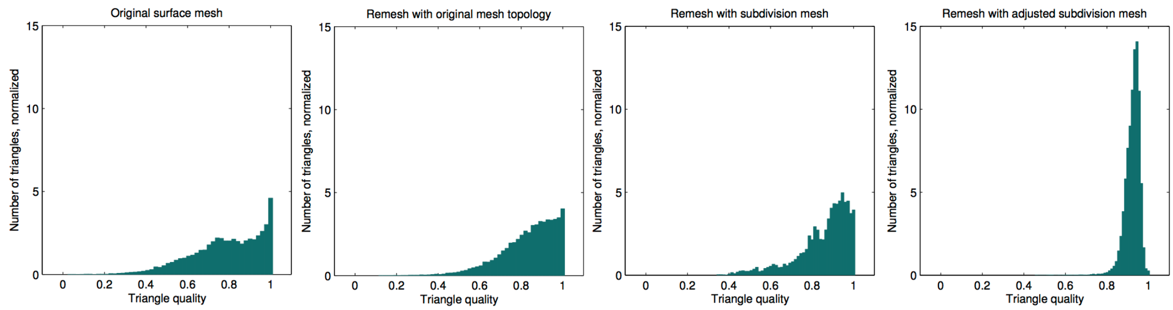

Fig. 18: Triangle quality of Foot

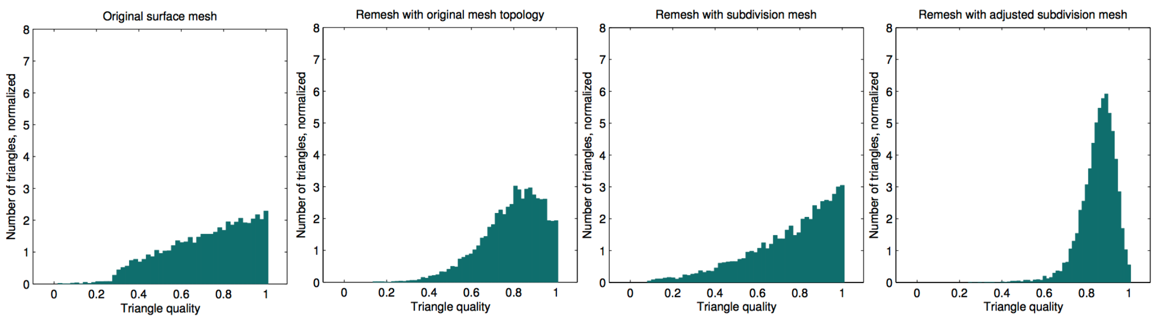

Fig. 19: Triangle quality of Hand

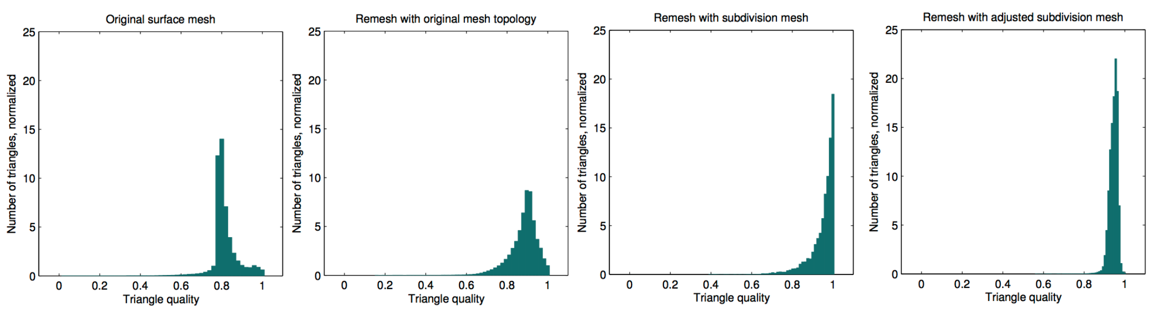

Fig. 20: Triangle quality of Venus

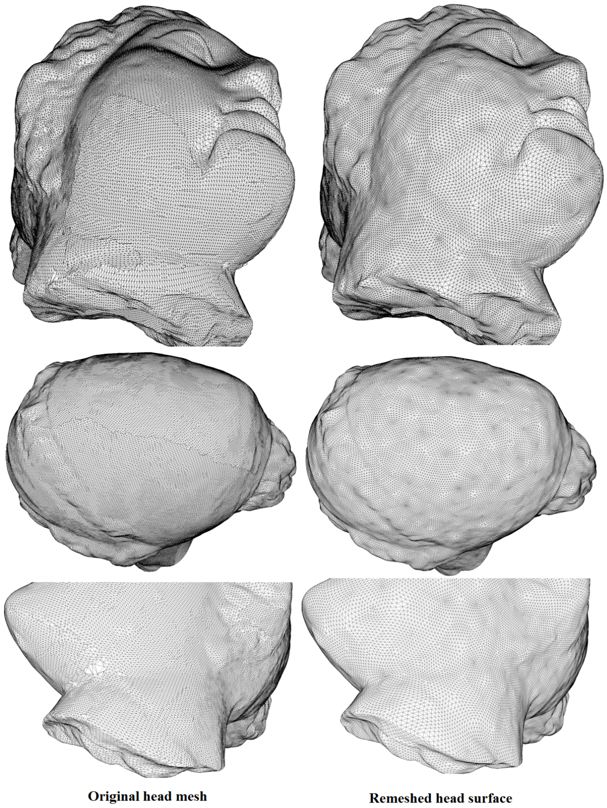

Fig. 15: Surface remeshing of the venus surface.

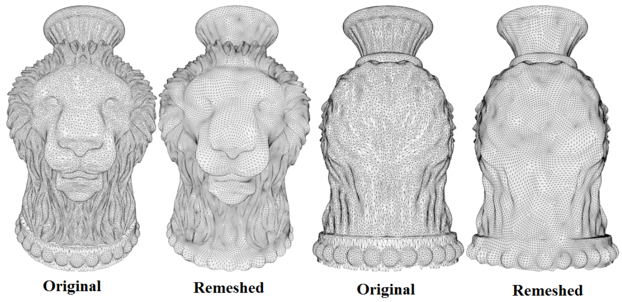

Fig. 16: Surface remeshing of the lion vase surface.

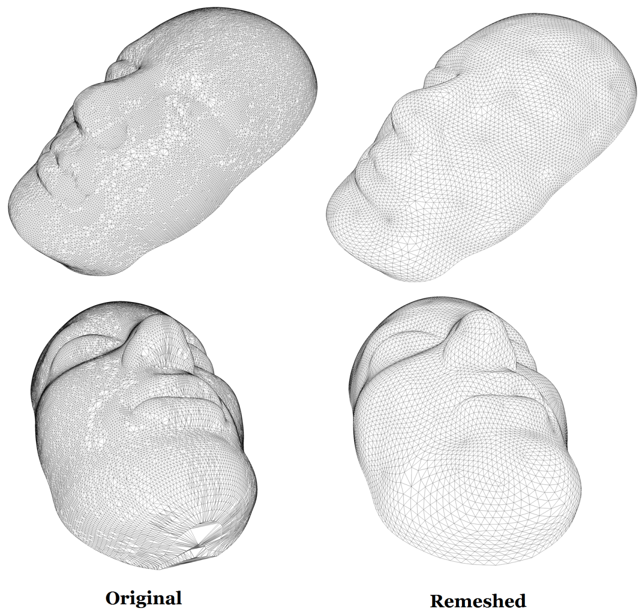

Fig. 17: Surface remeshing of the mask surface.

and M. Halle, *Conformal surface parameterization for texture mapping*. IEEE Trans. Visualization and Computer Graphics, 6(2):181189, 2000.

[22] X. Gu and S.T. Yau, *Computing conformal structures of surfaces*. Commun. Inform. Syst., vol. 2, no. 2, pp. 121-146, Dec. 2002.

[23] R. Lai, Z. Wen, W. Yin, X. Gu, and L.M. Lui, *Folding-Free Global Conformal Mapping for Genus-0 Surfaces by Harmonic Energy Minimization*. Journal of Scientific Computing, 2013. doi:10.1007/s10915-013-9752-6.

[24] F. Gardiner and N. Lakic, *Quasiconformal Teichmuller Theory*. American Mathematics Society, 2000.

[25] X. Gu, Y. Wang, T.F. Chan, P. Thompson, and S.T. Yau, *Genus zero surface conformal mapping and its application to brain surface mapping*. IEEE Transaction on Medical Imaging, 23:949-958, 2004.

[26] M. Jin, J. Kim, F. Luo and X. Gu. . IEEE Transaction on Visualization and Computer Graphics, 14(5), 1030-1043, 2008

[27] M. Jin, J. Kim, F. Luo and X. Gu. *Combinatorial Yamabe flow on surfaces*. Communication in Contemporary Mathematics, 6(5), 765-780, 2004

[28] Y.L. Yang R. Guo F. Luo S.M. Hu, X.F. Gu *Generalized Discrete Ricci Flow*. Computer Graphics Forum, 28(7), 20052014, 2009

[29] W. Zeng, L.M. Lui, L. Shi, D. Wang, W.C. Chu, J.C. Cheng, J. Hua, S.T. Yau, X.F. Gu. *Shape Analysis of Vestibular Systems in Adolescent Idiopathic Scoliosis Using Geodesic Spectra*. Medical Image Computing and Computer Assisted Intervation 13(3), 538-546, 2010.

[30] L.M. Lui, T.W. Wong, W. Zeng, X.F. Gu, P.M. Thompson, T.F. Chan and S.T. Yau. *Optimization of Surface Registrations Using Beltrami Holomorphic Flow*, Journal of Scientific Computing, 50(3), 557-585, 2012

[31] L.M. Lui, T.W. Wong, X.F. Gu, P.M. Thompson, T.F. Chan and S.T. Yau. *Hippocampal Shape Registration using Beltrami Holomorphic flow*, Medical Image Computing and Computer Assisted Intervention(MICCAI), Part II, LNCS 6362, 323-330 (2010)

[32] W. Zeng, L.M. Lui, F. Luo, T.F. Chan, S.T. Yau, X.F. Gu *Computing quasiconformal maps using an auxiliary metric and discrete curvature flow*. Numerische Mathematik, 121(4), 671-703, 2012

[33] L.M. Lui, K.C. Lam, T.W. Wong, X.F. Gu *Beltrami Representation and its applications to texture map and video compression*. arXiv:1210.8025 (http://arxiv.org/abs/1210.8025)

[34] W. Zeng and X. Gu. *Registration for 3D Surfaces with Large Deformations Using Quasi-Conformal Curvature Flow*. IEEE Conference on Computer Vision and Pattern Recognition (CVPR11), Jun 20-25, 2011, Colorado Springs, Colorado, USA.

[35] O. Weber, A. Myles, D. Zorin. *Computing Extremal Quasiconformal Maps*. Computer Graphics Forum, 31(5), 16791689 (2012)

[36] L.M. Lui, K.C. Lam, S.T. Yau, X.F. Gu *Teichmller extremal mapping and its applications to landmark matching registration*. arXiv:1211.2569(http://arxiv.org/abs/1210.8025)

[37] T.C. Ng, X.F. Gu, L.M. Lui *Teichmuller extremal map of multiply-connected domains using Beltrami holomorphic flow*. Journal of Scientific Computing, DOI 0.1007/s10915-013-9791-z (2013)

[38] L.M. Lui, X.F. Gu, S.T. Yau *Convergence analysis of an iterative algorithm for Teichmuller maps via harmonic energy optimization*. Mathematics of Computation (2014)

[39] Q. Du, V. Faber, M. Gunzburger *Centroidal Voronoi Tessellations: Applications and Algorithms*. SIAM Review 41 (4): 637676, doi:10.1137/S0036144599352836 (1999)

[40] A. Gersho *Asymptotically optimal block quantization*. IEEE Transactions on Information Theory 25, 4, 373380 (1979).

[41] G. Fejes Toth *A stability criterion to the moment theorem*. Studia Scientiarum Mathematicarum Hungarica 38, 1-4, 209224 (2001).

[42] P. Pébay and T. Baker *Analysis of triangle quality measures*. Mathematics of Computation, 72(244):18171839 (2003).